Shock Mitigation Studies in Voided Liquids for Fusion Chamber Protection

J. Oakley, M. Anderson, E. Marriott, J. Gudmundson,
K. Sridharan, V. Vigil, G. Rochau, R. Bonazza

November 2006

UWFDM-1319

Presented at the 17th ANS Topical Meeting on Fusion Energy, 13-15 November 2006, Albuquerque NM.

FUSION TECHNOLOGY INSTITUTE

UNIVERSITY OF WISCONSIN

MADISON WISCONSIN

Shock Mitigation Studies in Voided Liquids for Fusion Chamber Protection

J. Oakley, M. Anderson, E. Marriott, J. Gudmundson, K. Sridharan, V. Vigil, G. Rochau, R. Bonazza

Fusion Technology Institute
University of Wisconsin
1500 Engineering Drive
Madison, WI 53706

http://fti.neep.wisc.edu

November 2006

UWFDM-1319

Presented at the 17th ANS Topical Meeting on Fusion Energy, 13-15 November 2006, Albuquerque NM.

SHOCK MITIGATION STUDIES IN VOIDED LIQUIDS FOR FUSION CHAMBER PROTECTION

Jason Oakley[a], Mark Anderson[a], Ed Marriott[a], Jesse Gudmundson[a], Kumar Sridharan[a], Virginia Vigil[a], Gary Rochau[b], Riccardo Bonazza[a]

[a] *University of Wisconsin-Madison, 1500 Engineering Dr., Madison, Wisconsin, USA, 53706, manderson@engr.wisc.edu*
[b] *Sandia National Laboratories, PO Box 5800, Albuquerque, NM, USA, 87185*

A liquid pool, with and without void fractions, was subjected to dynamic compression testing in a vertical shock tube to model the bubbly-pool concept being considered for use in an inertial fusion energy reactor. Water and oil were used to model the FliBe coolant that collects at the bottom of the chamber and serves as first wall protection at that location. The experiments (shock strengths M=*1.4, 2.0, and 3.1) were conducted in atmospheric pressure argon, and argon was bubbled through the liquid to achieve void fractions of 5-15% in the 30.4 cm deep pool. Pressure measurements were taken in the pool at intervals of 2.54 cm to measure the effect void has on the pool compression and the compression wave traveling through the liquid. The presence of the gas voids in the liquid had a strong effect on the dynamic pressure loading but did not reduce the shock impulse significantly at the low and intermediate Mach numbers, but did exhibit a mitigating effect at the higher shock strength. A very high void fraction foam was also studied that resulted in a 22% reduction of the shock wave impulse.*

I. INTRODUCTION

Inertial fusion energy (IFE) power plant designs require a shock mitigation strategy to protect the chamber from repeated thermonuclear blasts. One proposed idea for a high repetition rate (6 Hz) moderate yield (350 MJ) conceptual power plant design is to use flowing liquid FliBe (F_2LiBe_4), either sheets or jets in a staggered configuration (with or without void), to protect the walls[1] and also to serve the functions of heat transfer and nuclear fuel breeding. Currently, there is an ongoing conceptual power plant design that instead utilizes high yield reactions (3 GJ) at a much lower repetition rate (0.1 Hz) and this provides a more challenging scenario where shock mitigation becomes more important. This new design, utilizing Z-pinch technology[2], is investigating the use of foam(s) to reap the benefits that a two-phase material can provide for shock mitigation[3]. The IFE target is suspended in the center of the chamber filled with low pressure gas (10-20 torr), inside of a hohlraum, by a conical recyclable transmission line (RTL). The interior of the RTL will be filled with solid foam FliBe to protect the top of the chamber, while a bubbly pool protects the bottom, and foamed liquid (two-phase) jets and sheets protect the side walls.

Previous shock tube investigations for chamber protection used solid aluminum foam as a model for the solid FliBe or PbLi foams in the RTL region. A series of low Mach number experiments (M=1.34) studied the shock attenuation properties of a single 2.54 cm layer suspended in a shock tube and also the effect of two layers separated by two different spacings[4]. The pressure behind the transmitted shock was reduced by 30% (compared with the incident shock) while the wave speed was reduced by 10% for the single layer configuration in argon initially at atmospheric pressure. The two layer configuration resulted in even greater pressure attenuation (50%) while the spacing between the layers was found to have little effect. The solid FliBe foam that would be incorporated into the RTL interior was modeled using two layers of 10.2 cm thick high-porosity aluminum foam of three different cell sizes subjected to a very strong M=6 shock wave[5]. The presence of the thick aluminum foam mitigated the shock wave; however, a very strong compression wave was transmitted through the foam. Energy absorption was found to be a function of cell size while the overall pressure load reduction was not, and larger pores were more effective at reducing the end-wall impulse.

The results reported here are for a new set of experiments concerned with understanding the shock mitigation effects of the bottom two phase pool in the Z-pinch reactor design, with varying shock strengths, M=1.4, 2.0, and 3.1, where the objectives are to study: 1) the attenuation of the shock wave as it passes through the bubble-filled, two-phase, pool, and 2) the impulse reduction observed when voids are present in the liquid. This data can then be used for initial code calculation verification and validation, before higher energy (*e.g.* high explosive) shock mitigation experiments are performed.

II. EXPERIMENT

The Wisconsin Shock Tube Laboratory[6] is utilized to conduct these shocked liquid pool studies. The 9.2 m long vertical shock tube has a large internal square cross section (25.4 cm sides), and is designed to withstand pressures of 20 MPa. Shock piezoelectric pressure transducers are mounted along a vertical wall of the shock tube to measure the transient nature of the pressure and the wave speeds. The driven section of the shock tube is filled with argon at atmospheric pressure, and nitrogen or helium is used in the driver to obtain the desired shock strength.

Figure 1 shows the experimental setup in the bottom of the shock tube. Gas flows through a fitting on the bottom of the shock tube into a cavity which remains slightly above atmospheric pressure. The argon flows through a Tyvek™ layer, whose presence is necessary to prevent water from filling up the argon cavity during experiment preparation, and then through a 1.27 cm thick aluminum foam[7,8]. The aluminum foam is an open-celled structure, Fig. 2, with a linear pore size of 0.64 mm and 40 pores per inch (ppi), and a porosity of $\phi = 0.89$, where $\phi = 1 - \rho_c / \rho_s$, $\rho_s = 2,700$ kg/m^3 (solid Al 6061 T6 density), and the cellular density is $\rho_c = 0.11\rho_s$. The compressive yield strength for the 40 ppi foam with this porosity has a plateau of $\sigma_{yc} = 3.0$ MPa and is relatively independent of the pore size[8]. The aluminum foam creates bubbles that are small, relative compared to the cross section of the shock tube (~5mm), and randomly distributed throughout the volume. An exhaust line is located above the pool's surface so that the pressure of the driven section of the shock tube remains at 1 atm. A solenoid-actuated valve for this line is pneumatically closed just prior to shock passage. PCB Piezoelectric shock pressure transducers sampling at 1 MHz are located along the center of one side of the shock tube with the faces flush mounted with the shock tube wall. There are four pressure transducers located above the pool to accurately measure the speed/pressure of the initial shock wave and the transducers are vertically spaced at intervals of 2.54 cm in the pool.

Figures 3 and 4 show argon bubbling up through water and oil in a mock-up of the shock tube test section having polycarbonate walls. The bubble population in the water is uniform across the width of the pool as well as the height. The turbulent nature of the bubble-bubble interaction while rising results in non-spherical gas bubbles at any moment in time, but over time, the bubbles in water may be considered spherical with an average diameter of D=5.6 mm with a standard deviation of 2.6 mm. Void fraction of gas was controlled by measuring the volumetric flow rate and levels up to 15% could be achieved. Numerous attempts to achieve higher void using

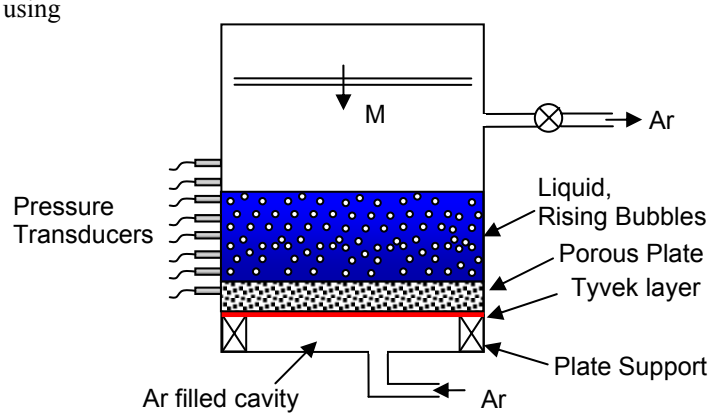

Fig. 1. Apparatus for simulating the shock mitigation response in the lower portion of the chamber.

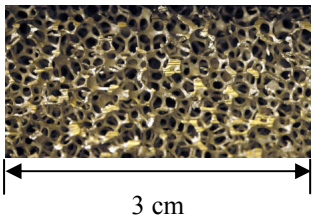

Fig. 2. Open cell-cell morphology of the 40 ppi aluminum foam used to create the bubble distribution.

different pore size foam (no effect, most likely because porosity remained constant); and a stainless steel porous plate instead of aluminum foam (resulted in very small bubbles and very low void fraction due to high head loss). The same 15% void fraction observed in the water was also seen in the mineral oil, however, the bubbly flow was much different than the flow in water, as seen in Fig. 4, and resulted in a bimodal bubble size distribution. The argon bubbling-up through the oil created a near-foam (in appearance) two-phase fluid, with many tiny bubbles of D<2 mm. In addition, there were a number of large-scale bubbles 15<D<30 mm that originated at the locations of small cap screws that were used to secure the porous plate to the support around the perimeter of the plate.

A final series of experiments were conducted at the high Mach number for shaving cream foam initially occupying the bottom 0.3 m of the shock tube. These experiments provide the contrast of a very low density, closed-cell foam, to the high-density water pool experiments.

II. SHOCK STRENGTH SCALING

Calculations of the shock strength following target ignition were carried out using BUCKY[9] to determine the pressure loading on the pool in the bottom of the reactor.

Pressure as a function of chamber radius is shown in Fig. 5 for a 3.05 GJ target yield in a chamber with an

Fig. 3. Water with 15% void fraction of argon in a mock-up of the shock tube test section with transparent walls-the width of the test section is 25.4 cm.

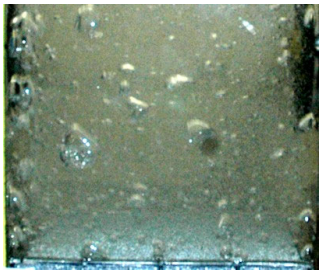

Fig. 4. Mineral oil with 5% void fraction of argon in a mock-up of the shock tube test section.

initial argon gas pressure of 12 mtorr (1.6 Pa). The pressure traces for t=115 and 900 ns show the regions of the target (DT, Be, CH, Au), argon, and FliBe (considered incompressible in the calculation). There is a compression wave moving radially outwards through the argon (shown at 115 ns), and when it reaches the FliBe, vaporization occurs (moving back into the argon, shown at 900 ns) which raises the local pressure above that of the argon. The compression wave that first reaches the FliBe raises the pressure to 1 J/cm^3 ($P_{contact}$=1 MPa) and then reaches a maximum of 23 J/cm^3 (P_{max}=23 MPa). For the shock tube experiments in atmospheric pressure argon, the shock strength required for $P_{contact}$=1 MPa is M=2.85, which would then result in an ideal P_{max}=4.2 MPa for a reflected shock wave off of an incompressible boundary. To reach the maximum argon pressure calculated from BUCKY (P_{max}=23 MPa) a shock strength of M=5.8 which is above the structural design limit of the shock tube. The pressure loading of the bubbly pool in the shock tube for the considered Mach numbers is on the same order as would be expected in the Z reactor, but not has high as the maximum pressure; however, the pressure ratios, and therefore Mach numbers, would be quite different.

IV. RESULTS

Prior to conducting the two-phase fluid experiments, a series of calibration runs were performed to quantify the shock wave and verify the operability of the pressure transducers. The data collected from the experiments include pressure traces and material surface corrosion. This campaign consisted of a total of 52 experiments covering three Mach numbers, and the response of

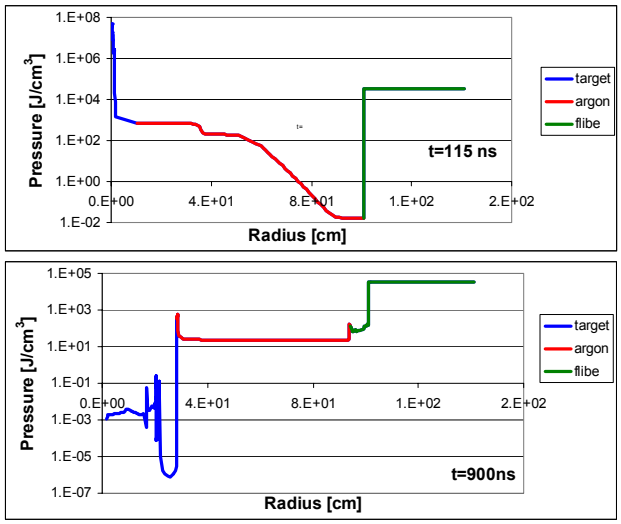

Fig. 5. Pressure as a function of radius for the line of sight from the target to the coolant pool at the bottom of the chamber calculated using BUCKY.

three different two-phase fluids of: water/argon, oil/argon, and shaving cream foam.

Three shock strengths were chosen for these studies and the properties are listed in Table 1. The initial shock wave speed, W_i, is for the listed Mach number in argon at standard temperature and pressure; the reflected shock wave speed, W_r, is the calculated speed for the reflection off an incompressible surface; the gas velocity behind the incident shock is u_2; and the pressure, P, with subscripts 1, 2, and 5 are the initial pressure, the pressure behind the incident shock wave, and the pressure behind the reflected shock wave, respectively.

TABLE I. The experimental parameters, for argon, calculated from 1-D gasdynamics.

M	W_i (m/s)	W_r (m/s)	u_2 (m/s)	P_1 (MPa)	P_2 (MPa)	P_5 (MPa)
1.4	456	343	170	0.101	0.227	0.453
2.0	646	405	363	0.101	0.482	1.52
3.1	1,001	554	672	0.101	1.19	5.26

Pressure traces from the same transducer for each of the void fraction pools are shown in Fig. 6 for some low Mach number water pool experiments. The pressure in the pool without a void fraction resemble the P_5 plateau that would be observed for a shock wave reflected off a rigid surface, this is indicative of the relative incompressibility of the water compared with the argon. At longer times, t>1 ms in Fig. 6(a), the pressure trace resembles the P_5 plateau for each of the void fractions. The early time behavior is quite variable for the different void fractions as seen in Fig. 6(b). When there is no void fraction, a near-discontinuity pressure rise is observed as

would be expected for a shock wave (not traveling through the water but reflecting off the surface of the water back into the argon); however, the presence of the argon bubbles in the pool has a strong effect on the pressure traces and oscillations are observed in the traces before leveling out at later times. Each of the pressure traces for void fractions of 5, 10, and 15% argon show an initial compression that is not discontinuous, and is the response of the argon bubbles in the pool compressing. The time when the bubbles in the pool have reached maximum compression corresponds to the time of peak pressure; this is then followed by an expansion of the bubbles which reduces the pressure. Cyclic compression and expansion continues during the early times and the measured oscillations reflect this cycling, and not necessarily reverberating pressure waves in the bubbly pool. There is some higher frequency oscillatory content in the 5 and 15% argon void fraction traces which is most likely due to a proximity effect for a single bubble being closer to the transducer face (circular, 5 mm diameter) and therefore responding slightly different than the overall, average, pool response.

Results for the impulse calculations are given in Table 2. The impulse time (t_I) is chosen as the time it takes an unattenuated shock wave to travel through the distance of the pool depth, h=0.3048 m. The impulse interval begins when a pressure is first registered by the transducer. The impulse time goes down with increasing shock strength but the impulse goes up due to the stronger effect of the higher shock strength's pressure rise. Although very different behavior is seen in individual pressure traces, the presence of argon voids in the pool has little, if no, effect on the calculated impulse at the low and medium Mach number experiments. At the low and medium Mach number experiments, the shock wave speed is well below the sound speed in water (1,500 m/s at STP) and the pool shows a primarily incompressible response to the shock loading- even though the bubbles are compressing within the pool. A pool with a much higher void fraction (*e.g.* foam) would be expected to show a different response, with the increased void fraction resulting in an impulse reduction. A 12% reduction was observed in the high Mach number experiments, which indicates the significance of compressibility of the argon voids in the pool. The wave speed of the high Mach number experiments is approaching that of the acoustical speed in pure water, thus, the response of the bubbly pool is that of a two-phase mixture and is no longer purely dominated by the incompressible nature of the water as observed in the lower shock strength experiments. Also, heating of the pool due to compression of the bubbles will affect the sound speed during the shock wave interaction.

Experiments to study the response of a mineral oil pool with argon bubbles were only conducted at the higher void fraction (15%) and the high Mach number. An even greater impulse reduction was seen in this two-phase pool as the impulse dropped from 131 N-s to

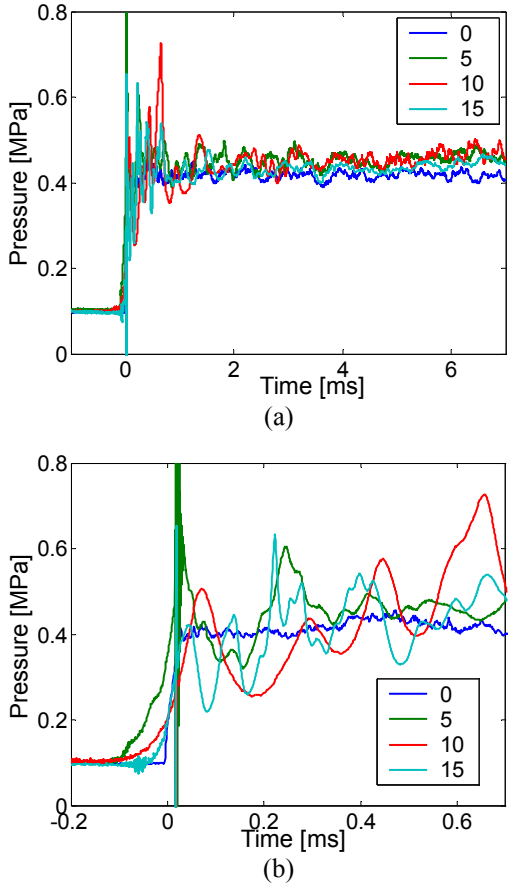

Fig. 6. Pressure traces for a M=1.4 experiment from a transducer located 3.5 cm below the surface of the pool for 0, 5, 10 and 15% argon void fraction: (a) long-time, (b) short-time.

TABLE II. Impulse measurements for the pool with argon bubbles.

M	I_0 [N s]	I_5 [N s]	I_{10} [N s]	I_{15} [N s]	t_I [ms]
1.4	13.2	14.9	14.5	13.1	0.67
2.0	40.3	39.8	38.2	41.7	0.47
3.1	82.0	-	-	72.0	0.31

86 N-s (34%). The greater reduction in impulse may be partially attributed the lower bulk modulus of oil compared to water (resulting in a lower sound speed, 1,300 m/s at STP); however, given the magnitude, it is more likely due to the very different bubble distribution of the argon in the oil, particularly the smaller bubbles that resulted in a more foamy liquid.

Using the bubbly-pool configuration, only a low gas fraction two-phase pool could be achieved. Shaving

cream foam was used to contrast the behavior of a high density pool to very low density foam which also has a closed-cell structure (density of 66 kg/m^3 and an estimated gas void fraction of 94%). The bottom 0.3 m of the shock tube was filled with the foam and experienced no visible settling from the time of preparation to the time of shock arrival (typically less than 30 minutes). A pressure trace result for an M=3.1 experiment is shown in Fig. 7 and, for comparison, the reference is a shock wave in the gas (air). In the pure gas trace, the shock wave initially steps up the pressure to 1.2 MPa (P_2) and then at 0.8 ms the pressure is stepped up to 5.3 MPa (P_5). After 1.5 ms it is clear that the rarefaction from the shock tube driver has expanded down to the pressure transducer location which lowers the pressure in an exponentially decaying fashion. When the shaving cream foam is present, the response is much different, with the initial pressure rise showing fast compression, although not stepped as in the shock wave case, which is between the P_2 and P_5 pressures of the shock wave in the argon. At the later times, during the rarefaction phase, the exponential decay of the pressure is the same in both cases. An arbitrary time of 2 ms was chosen for comparing the impulse between the foam and no-foam cases and a reduction from 441 N-s to 344 N-s was observed, a 22% reduction.

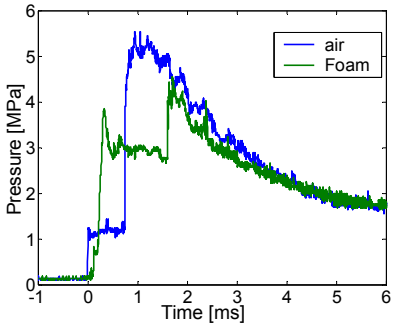

Fig. 7. Pressure traces from a transducer located 0.24 m below the surface of the shaving cream foam.

IV. CONCLUSIONS

A series of shock tube experiments were conducted to model the FliBe pool response in the Z-chamber. Only low gas void fraction (5-15%) could be achieved by bubbling argon through an aluminum foam plate beneath a pool of liquid, either water or oil. Although the pressure traces in pools with gas bubbles exhibited much different behavior than the measured traces for pure gas or pure liquid, the overall effect on impulse was not observed at the low and medium (M=1.4 and 2.0) experiments. The shock mitigation effect of the bubbly pool was observed in both the water and oil pools in the higher shock strength experiments (M=3.1) with the bubble distribution playing a role in the amount of observed mitigation to the impulse- smaller bubbles resulted in a foamy-like liquid with a greater impulse reduction. A very high gas void fraction shaving cream foam resulted in a 22% reduction in impulse for the high Mach number experiments which indicates that more experiments need to be done in the intermediate void fraction regimes to reach a conclusion about the optimum concentration of gas to liquid for shock mitigation.

ACKNOWLEDGMENTS

This work sponsored by the Z-pinch IFE program, U.S. Department of Energy and Sandia National Laboratories, contract number 426334.

REFERENCES

1. R. MOIR, "HYLIFE – II: A molten-salt inertial fusion energy power plant design-Final report," Fusion Technology, Vol. 25, pp. 5-25 (1994).
2. C. OLSON *et al*., "Development path for Z-pinch IFE," Fusion Science and Technology, Vol. 47, pp. 633-640 (2005).
3. K. KITAGAWA, M. YOKOYAMA and M. YASUHARA, "Attenuation of shock waves by porous materials,' 24th International Symposium on Shock Waves Proceedings, Beijing, China, Paper 2692 (2004).
4. M. H. ANDERSON, J. G. OAKLEY, P. MEEKUNNASOMBAT and R. BONAZZA, "The dynamics of a shock wave and aluminum foam layer interaction," 25th International Symposium on Shock Waves Proceedings, Bangalore, India, Paper 1197, (2005).
5. M. H. ANDERSON, J. G. OAKLEY, V. VIGIL, S. RODRIGUEZ and R. BONAZZA, "Shock mitigation studies of solid foams for Z-Pinch chamber protection," report following Z-Pinch IFE workshop, Sandia National Laboratories, Albuquerque, NM, Aug 1-2, 2005.
6. M. H. ANDERSON, B. P. PURANIK, J. G. OAKLEY, P. W. BROOKS and R. BONAZZA, "Shock tube investigation of hydrodynamic issues related to inertial confinement fusion," Vol. 10, No. 5, pp. 377-387, (2000).
7. L. J. GIBSON and M. F. ASHBY, "Cellular solids, structure & properties," Pergamon Press, Oxford, 1988.
8. Energy Research and Generation, Inc. "Duocell Aluminum Foam Brochure," 900 Stanford Ave., Oakland, CA, (510) 658-9785.
9. T. A. HELTEMES, E. P. MARRIOTT, G. A. MOSES and R. R. PETERSON, "Z-pinch (LiF)2-BeF2(FliBe) preliminary vaporization estimation using the BUCKY 1-D radiations hydrodynamics code," 21st IEEE/NPSS Symposium on Fusion Energy (SOFE), 26-29 Sep. 2005, Knoxville, TN.